ARTHRITIS & RHEUMATOLOGY
Vol. 68, No. 10, October 2016, pp 2476–2486
DOI 10.1002/art.39732
© 2016, American College of Rheumatology

Interleukin-23–Dependent γ/δ T Cells Produce Interleukin-17 and Accumulate in the Enthesis, Aortic Valve, and Ciliary Body in Mice

Annika Reinhardt,[1] Tetyana Yevsa,[1] Tim Worbs,[1] Stefan Lienenklaus,[1] Inga Sandrock,[1] Linda Oberdörfer,[1] Thomas Korn,[2] Siegfried Weiss,[1] Reinhold Förster,[1] and Immo Prinz[1]

Objective. **The spondyloarthritides (SpA) are a group of rheumatic diseases characterized by ossification and inflammation of entheseal tissue, the region where tendon attaches to bone. Interleukin-23 (IL-23) is involved in the pathogenesis of SpA by acting on IL-23 receptor (IL-23R) expressed on enthesis-resident lymphocytes. Upon IL-23 binding, CD3+CD4−CD8− tissue-resident lymphocytes secrete IL-17A and IL-22, leading to inflammation, bone loss, and ossification. Knowledge about enthesis-resident lymphocytes remains fragmentary, and the contribution of entheseal γ/δ T cells in particular is not clear. This study was undertaken to investigate the presence of γ/δ T cells in the enthesis.**

Methods. **We used 2-photon microscopy and flow cytometry to analyze entheseal lymphocytes from C57BL/6, *Tcrd-H2BeGFP*, *Rorc-GFP*, and *IL-23R-eGFP* mice. To analyze entheseal γ/δ T cells in IL-23–induced inflammation, *Tcrd-H2BeGFP* mice were crossed with mice of the susceptible B10.RIII background. Hydrodynamic injection of IL-23 minicircle DNA was performed for overexpression of IL-23 and induction of inflammation. Light-sheet fluorescence microscopy was used to visualize arthritic inflammation.**

Results. **Activated Vγ6+CD27− γ/δ T cells were abundant in uninflamed entheseal tissue and constituted the large majority of retinoic acid receptor–related orphan nuclear receptor γt (RORγt)+IL-23R+ enthesis-resident lymphocytes. Fetal thymus–dependent γ/δ T cells were the main source of IL-17A at the enthesis. Under inflammatory conditions, γ/δ T cells increased in number at the Achilles tendon enthesis, aortic root, and adjacent to the ciliary body.**

Conclusion. **Entheseal γ/δ T cells are derived from fetal thymus and are maintained as self-renewing tissue-resident cells. As main IL-17A producers within tissues exposed to mechanical stress including enthesis, γ/δ T cells are key players in the pathogenesis of IL-23–induced local inflammation.**

The spondyloarthritides (SpA) are a group of rheumatic diseases that include reactive arthritis, psoriatic arthritis, and inflammatory bowel disease (IBD)–associated arthritis as well as ankylosing spondylitis (AS), the prototype of SpA. SpA mainly manifests as inflammation and ossification of entheseal tissue, the region where tendon fibers or ligaments attach to bone. In humans, the disease entity primarily affects the axial skeleton, leading to chronic back pain and diminished mobility, but it also comprises extraarticular manifestations (1), such as psoriasis, gut inflammation, uveitis, and aortitis (2).

Genome-wide association studies identified a number of genes that confer susceptibility to SpA (3), including HLA–B27, endoplasmic reticulum aminopeptidase 1 (ERAP-1) and ERAP-2, and particularly interleukin-23 receptor (IL-23R). Suggesting a common pathogenic mechanism, a similar linkage to IL-23R polymorphisms was identified in psoriasis (4) and IBD (5), which are often associated with axial arthritis and enthesitis. Within the last few years, a key role of IL-23 in the pathogenesis of

Supported by the Deutsche Forschungsgemeinschaft SPP1468 ImmunoBone (grant DFG PR727/5-1 to Dr. Prinz). Ms Reinhardt is a scholar of the Infection Biology (ZIB) PhD program within the Hannover Biomedical Research School.

[1]Annika Reinhardt, MSc, Tetyana Yevsa, Dr. rer. nat., Tim Worbs, Dr. rer. nat., Stefan Lienenklaus, Dr. rer. nat., Inga Sandrock, Dr. rer. nat., Linda Oberdörfer, Siegfried Weiss, Dr. rer. nat., Reinhold Förster, Prof. Dr. med. vet., Immo Prinz, Prof. Dr. rer. nat.: Hannover Medical School, Hannover, Germany; [2]Thomas Korn, Prof. Dr. med.: Klinikum rechts der Isar, Technische Universität München and Munich Cluster of Systems Neurology (SyNergy), Munich, Germany.

Address correspondence to Immo Prinz, Prof. Dr. rer. nat., Institute of Immunology, Hannover Medical School, Carl-Neuberg-Strasse 1, 30625 Hannover, Germany. E-mail: prinz.immo@mh-hannover.de.

Submitted for publication December 21, 2015; accepted in revised form April 21, 2016.

SpA was suggested (6). Data collected from HLA–B27–transgenic rats indicated possible links between HLA–B27 and the IL-23 cytokine pathway, since HLA–B27 misfolding led to increased IL-23 secretion by macrophages (7) and lamina propria mononuclear cells (8), thereby likely conferring susceptibility to SpA. Indeed, elevated levels of IL-23 were identified in serum (9) and in intestinal biopsy samples (10) from AS patients.

Recently, using an IL-23–dependent mouse model of experimental SpA, Sherlock and colleagues demonstrated that IL-23 is specifically involved in the induction of entheseal inflammation by acting on enthesis-resident IL-23R+CD3+CD4−CD8− lymphocytes (11). Upon IL-23 binding, entheseal CD3+ lymphocytes secreted high amounts of IL-17 and IL-22, inducing typical features of SpA, such as enthesitis and new bone formation (11). In fact, elevated levels of serum IL-17 (9) and IL-17– and IL-22–producing peripheral blood CD4+ T cells have been observed in AS patients (12). Notably, patients with enthesitis-related arthritis also displayed increased frequencies of synovial fluid IL-17 (13).

To date, only a few analyses of entheseal inflammatory infiltrates from SpA patients have been performed. So far, accumulations of either CD3+ T cell (14), macrophage (15), or mast cell (16) have been described. In this study, we further characterized the elusive enthesis-resident CD4−CD8− T cell population that was first identified in mice by Sherlock and colleagues (11). In contrast to the majority of α/β T cells, γ/δ T cells are not major histocompatibility complex−restricted and lack surface expression of the co-receptors CD4 and CD8. They are scarce in secondary lymphoid organs, but represent a main lymphocyte population within epithelial or mucosal tissues such as skin or intestine. Therefore, in this study we hypothesized and investigated to what extent γ/δ T cells constituted the entheseal lymphocyte population. In humans, an enrichment of IL-17−producing IL-23R+ γ/δ T cells was recently identified in the peripheral blood of patients with AS (17) or enthesitis-related arthritis (13). Thus, it was likely that γ/δ T cells are enthesis-resident key producers of IL-17A.

Using *Tcrd-H2BeGFP* reporter mice, we identified and characterized a novel population of mouse enthesis-resident γ/δ T cells that readily produce IL-17A at this specific anatomic site. We showed that in mice overexpressing IL-23, entheseal γ/δ T cells accumulate at the Achilles tendon enthesis, the aortic root, and the eye.

MATERIALS AND METHODS

Mice. B10.RIII-*H2*^{r} *H2-T18*^{b}/(71NS)SnJ (here B10.RIII) and C57BL/6 mice were purchased from The Jackson Laboratory. C57BL/6-*Trdc*^{tm1Mal}/J (here *Tcrd-H2BeGFP*) mice (18) encoding an internal ribosome entry site (IRES) and a human histone (H2B) fused to enhanced green fluorescent protein (EGFP) downstream of the *Tcrd* constant region, C57BL/6-Tg(*Rorc-EGFP*)1Ebe (here *Rorc-GFP*) mice (19) expressing EGFP under control of the *Rorc* locus on a bacterial artificial chromosome, and C57BL/6-*Il23r*^{tm1Kuch} (here *IL-23R-eGFP*) mice (20) were used. As opposed to *Tcrd-H2BeGFP* and *Rorc-GFP* mice, which allow normal *Tcrd* and *Rorc* expression unaffected by the transgene, *IL-23R-eGFP* mice contain an IRES−EGFP cassette introduced into an exon of the *IL-23r* locus, causing intragenic deletion. Homozygous mice are unresponsive to signals via the IL-23R, whereas the heterozygous mice that were used in this study allow normal signaling and detection of IL-23R expression. To generate Indu-*Rag1* × *Tcrd-H2BeGFP* mice with lymphocyte development inducible by tamoxifen (21), *Rag1*$^{-/-}$ mice (22) were crossed to the *Tcrd-H2BeGFP* strain. Mice were injected with tamoxifen between 8 and 16 weeks of age. For induction of IL-23−dependent inflammation, *Tcrd-H2BeGFP* mice were crossed to the B10.RIII background for 5 generations (B10.*Tcrd-H2BeGFP*). All animals were maintained under specific pathogen−free conditions in the Central Animal Facility at Hannover Medical School. Mice were analyzed at 6−12 weeks of age. Experiments were carried out according to institutional guidelines approved by the Lower Saxony State Office for Consumer Protection and Food Safety animal care and use committee.

Antibodies. Antibodies against CD3 (145-2C11), T cell receptor β (TCRβ; REA318), CD44 (IM7.8.1), and TCRγ/δ (GL-3) were purchased from Miltenyi Biotec. Antibodies against CD27 (LG.3A10), Ly6C (HK1.4), Vγ1 (2.11), and Vγ4 (UC3-10A6) were obtained from BioLegend, antibodies against CD45.2 (104), IL-17A (eBio17B7), interferon-γ (IFNγ; XMG1.2), and rat IgM (RM-7B4) were from eBioscience. Anti-CCR6 (140706) and anti−IL-23R (078-1208) were purchased from BD PharMingen. Antibodies against CD4, CD8, CD62L, and Vγ6 (17D1) were produced from rat hybridoma cell lines. The 17D1 antibody recognizing Vγ5 and Vγ6 when combined with anti-TCRγ/δ (GL-3) has been described previously (21,23).

Preparation of entheseal cells for flow cytometric analysis. Entheseal cells were isolated as previously described (11), with the following minor modifications. Tissue was digested for 2 hours in RPMI (Invitrogen) containing 10% fetal calf serum, 3 mg/ml collagenase D (Roche), and 112 μg/ml DNase (Roche). Digestion was stopped by adding 0.02*M* EDTA during the last 15 minutes. Dead cells were either stained with DAPI or Zombie Aqua (BioLegend). For intracellular cytokine staining, cells were incubated for 3 hours with phorbol myristate acetate (PMA) (50 ng/ml; Calbiochem), ionomycin (2 μg/ml; Invitrogen), and brefeldin A (1 μg/ml; Sigma) or overnight in the presence of IL-23 (10 ng/ml; R&D Systems) supplemented with brefeldin A (1 μg/ml; Sigma) for the last 3 hours. Cells were fixed and permeabilized with Cytofix/Cytoperm (BD Biosciences) according to the manufacturer's instructions.

IL-23 minicircle−induced inflammation. The IL-23−encoding vector RSV-mIL23-MN100A (MC-Easy Minicircle Production Kit) was obtained from BioCat. Using standard molecular techniques, 331 and 425 basepairs within the IL-23p19 and IL-12/IL-23p40 subunits, respectively, were excised to obtain IL-23−deficient control vector DNA. Minicircle induction was performed according to the manufacturer's instructions, with minor modifications. Briefly, 10 ml Luria-Bertani (LB) medium containing 50 μg/ml kanamycin was inoculated with glycerol stock

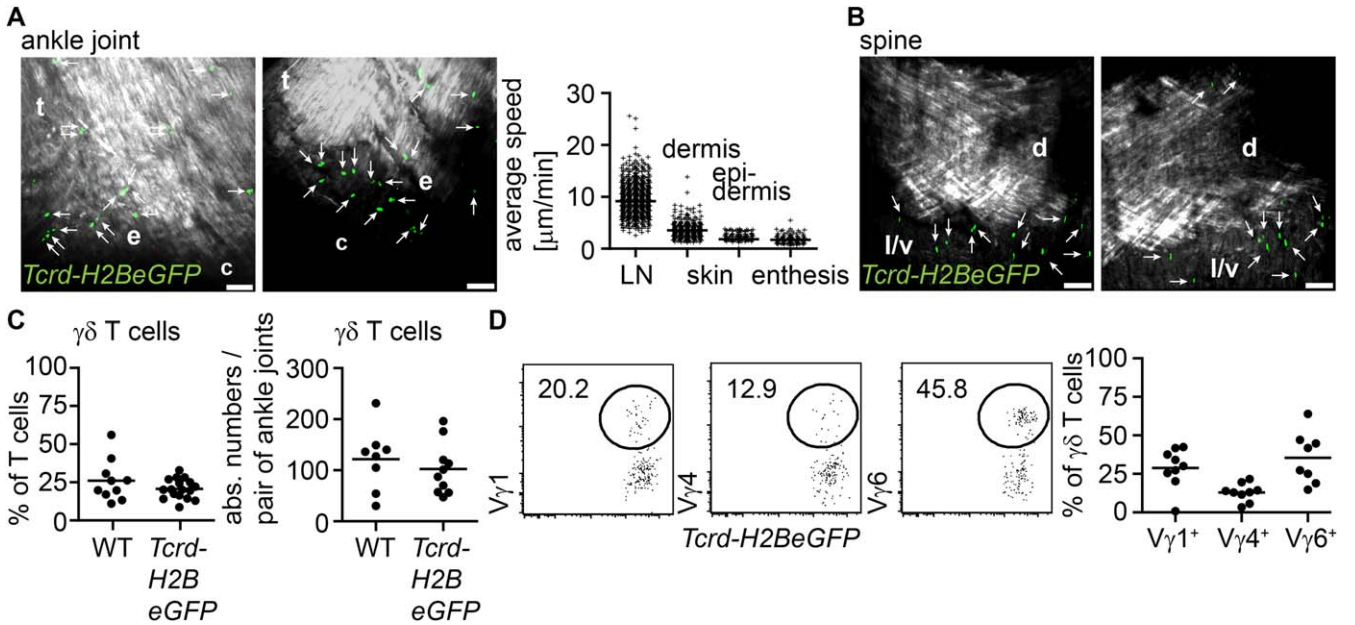

Figure 1. Vγ6+ γ/δ T cells reside within entheseal tissues. **A**, Posterior views of mouse ankle joints analyzed ex vivo (left) and in vivo (middle), obtained by 2-photon microscopy, and average speeds of lymph node (LN)−resident, skin-resident, and entheseal γ/δ T cells (right). Symbols represent individual cell tracks; horizontal lines show the median average tracking speed. Data on LN and skin are from 2 independent experiments; data on enthesis are from 3 independent experiments. **B**, Anterior views of *Tcrd-H2BeGFP* mouse vertebrae analyzed ex vivo, obtained by 2-photon microscopy. In **A** and **B**, **arrows** indicate γ/δ T cells, green indicates *Tcrd-H2BeGFP*, and white indicates collagen (second harmonic signal). **t** = tendon; **e** = enthesis; **c** = calcaneus; **d** = disc; **l/v** = ligament/vertebra. Bars = 50 μm. Images are representative of at least 3 mice per joint. **C**, Frequency of γ/δ T cells among T cells (left) and absolute (abs.) numbers of γ/δ T cells (right), as determined by flow cytometric analysis of γ/δ T cells isolated from the ankle joints of C57BL/6 wild-type (WT) and *Tcrd-H2BeGFP* mice. Data on WT mice are from 3 independent experiments; data on *Tcrd-H2BeGFP* mice are from 7 independent experiments. **D**, Frequencies of entheseal γ/δ T cells expressing Vγ1, Vγ4, or Vγ6, as determined by flow cytometric analysis of γ/δ T cells isolated from the ankle joints of C57BL/6 WT and *Tcrd-H2BeGFP* mice. Dot plots depict pooled data from 2 mice representative of 8 independent experiments. In **C** and **D**, symbols represent individual mice; horizontal lines show the mean.

bacteria and incubated overnight at 30°C with shaking. LB/kanamycin (440 ml) was inoculated overnight with 10 ml of bacterial culture and grown until the optical density at 600 nm reached 0.3. L-arabinose was then added in a final concentration of 1%. Bacteria were further grown for up to 3 hours, and minicircle DNA was isolated. Before in vivo application of minicircle DNA vector technology, functionality of control and IL-23 minicircle DNA was analyzed in vitro (see Supplementary Methods and Supplementary Figure 1, available on the *Arthritis & Rheumatology* web site at http://onlinelibrary.wiley.com/doi/10.1002/art.39732/abstract). B10.*Tcrd-H2BeGFP* mice were hydrodynamically injected in the tail vein with 20 μg of purified minicircle DNA diluted in Ringer's solution in a final volume of 10% per body weight. In vivo transgene expression was monitored by measuring serum IL-23 protein levels using enzyme-linked immunosorbent assay (ELISA), performed according to the manufacturer's instructions (Mouse IL-23 ELISA MAX Deluxe Set; BioLegend). Mice were killed 21−30 days after injection.

Two-photon microscopy. For ex vivo imaging of ankle joints and spines, mice were killed and perfused. Skin and organs were removed, and the entheseal regions were dissected carefully. Joints were immobilized in a petri dish using tissue adhesive. For in vivo imaging, mice were anesthetized and mounted onto a 37°C heating plate. The Achilles tendon entheses were dissected carefully to visualize entheseal γ/δ T cells. For in vivo imaging of skin-resident γ/δ T cells, a coverslip was placed on the ventral side of the ear. To analyze lymph node−resident γ/δ T cells, the inguinal lymph nodes were isolated and immobilized in a custom-built imaging chamber using tissue adhesive. Lymph nodes were superfused with oxygenated medium (95% O_2/5% CO_2) supplemented with 1% penicillin/streptomycin. Imaging was performed with a TriM Scope (LaVision BioTec) equipped with an upright Olympus BX51 microscope with a 20×/0.95 water immersion objective and a pulsed Ti sapphire infrared laser (Mai Tai; Spectra-Physics) turned to 920 nm. Fields of view of 500 μm (x) × 500 μm (y) × 114−186 μm (z) were acquired using a z-step size of 3−6 μm. Data analysis was performed using Imaris software 7.7.2 (Bitplane).

Light-sheet fluorescence microscopy. Sample preparation was adapted from the method of Ertürk and colleagues (24). Mouse joints were collected, fixed in phosphate buffered saline (PBS) with 2% paraformaldehyde and 30% sucrose, and subsequently washed in PBS. Tissues were dehydrated in 50% tetrahydrofuran (THF) for 10 hours, in 75% THF overnight, and twice in 100% THF for at least 5 hours each. Samples were cleared overnight in dibenzyl ether and imaged after clearing was completed. Images were acquired using a light-sheet fluorescence microscope (Ultramicroscope II; LaVision BioTec) equipped with an sCMOS camera (Andor Neo) and a 2×/0.5

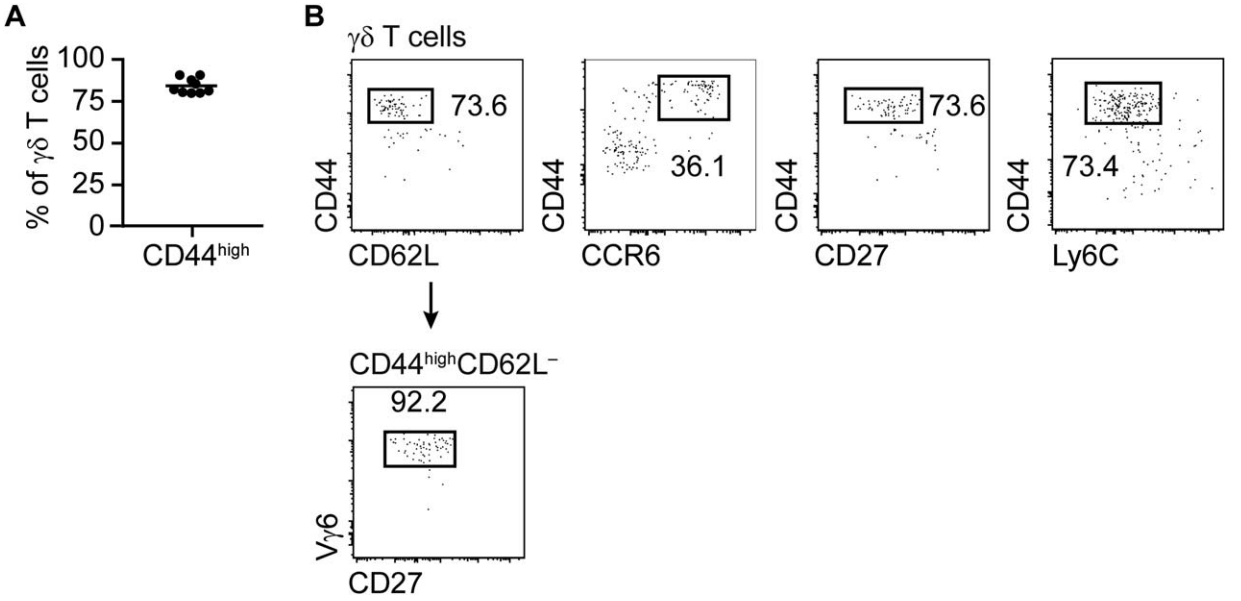

Figure 2. Preactivated effector cells dominate the pool of enthesis-resident γ/δ T cells. Results of flow cytometric analysis of γ/δ T cells isolated from the ankle joints of *Tcrd-H2BeGFP* mice are shown. **A**, Frequency of $CD44^{high}$ cells among entheseal γ/δ T cells. Symbols represent individual mice; horizontal line shows the mean. Data from 3 independent experiments are shown. **B**, Top, Expression of CD44, CD62L, CCR6, CD27, and Ly6C on entheseal γ/δ T cells. Bottom, Frequency of Vγ6+CD27− cells among entheseal $CD44^{high}CD62L-$ γ/δ T cells. Dot plots depict pooled data from 2 or 3 mice representative of at least 3 independent experiments.

objective lens (Olympus). Three-dimensional projections were analyzed with Imaris software 7.7.2 (Bitplane).

Micro−computed tomography (micro-CT). Micro-CT was performed using an Inveon micro-CT scanner (Siemens) equipped with Inveon Acquisition Workplace software 1.5 (Siemens). Data were acquired using filter 2 with a photon energy of 80 kV, a current of 500 μA, and an exposure time of 200 msec. Data reconstruction was performed using bilinear interpolation, the Shepp-Logan reconstruction filter, and the beam-hardening coefficient for standard soft tissue. Image analysis was performed using Inveon Research Workplace software 2.3 (Siemens).

Histologic analysis. Mouse organs were collected and frozen in Tissue-Tek OCT compound (Sakura) on dry ice. Eight-micrometer cryosections were cut using a cryomicrotome (CM3050; Leica), and sections were fixed with acetone. Organs were stained with either hematoxylin and eosin or anti-CD3 (17A2; made in-house) and anti-CD45 (30-F11; eBioscience). Images were acquired using a motorized upright Olympus BX61 fluorescence microscope equipped with a 10×/0.4 objective (UPlanSApo; Olympus), 2 cameras (ColorView IIIu and F-View II; Olympus), and cellSens software 1.12 (Olympus).

Statistical analysis. Statistical analyses were performed using GraphPad Prism software.

RESULTS

Tissue-resident γ/δ T cells in the enthesis. In this study, we sought to investigate the presence of γ/δ T cells in mouse entheseal tissues. To this end, we first performed 2-photon microscopy of the ankle joints of naive *Tcrd-H2BeGFP* reporter mice (Figure 1A). The *Tcrd-H2BeGFP* reporter mouse model enables direct identification of γ/δ T cells based on their intense nuclear fluorescence (18). Ex vivo imaging of the Achilles tendon insertion into the posterior calcaneus allowed us to visualize numerous entheseal γ/δ T cells (Figure 1A). We further monitored the motility of enthesis-resident γ/δ T cells in *Tcrd-H2BeGFP* ankle joints (Figure 1A). As opposed to motile lymph node−resident or slow tissue-scanning dermal γ/δ T cells, but similar to dendritic epidermal γ/δ T cells, entheseal γ/δ T cells appeared to be tethered within their anatomic niches and did not exhibit migratory capacities (Figure 1A and Supplementary Video 1, available on the *Arthritis & Rheumatology* web site at http://onlinelibrary.wiley.com/doi/10.1002/art.39732/abstract). Importantly, γ/δ T cells were also highly present in spinal entheses, specifically located where intervertebral discs attach to vertebral end plates (Figure 1B).

Next, entheseal lymphocytes from the ankle joints of naive *Tcrd-H2BeGFP* mice were isolated and compared to control lymphocytes from C57BL/6 (wild-type) mice by flow cytometry. Notably, γ/δ T cells represented ~25% of enthesis-resident T cells in both strains, while 75% were α/β T cells (Figure 1C and Supplementary Figures 2A and B, available on the *Arthritis & Rheumatology* web site at http://onlinelibrary.wiley.com/doi/10.1002/art.39732/abstract). Compared to spleen or lymph nodes, in which γ/δ T cells make up only ~1−2% of CD3+ T cells (25), the enthesis

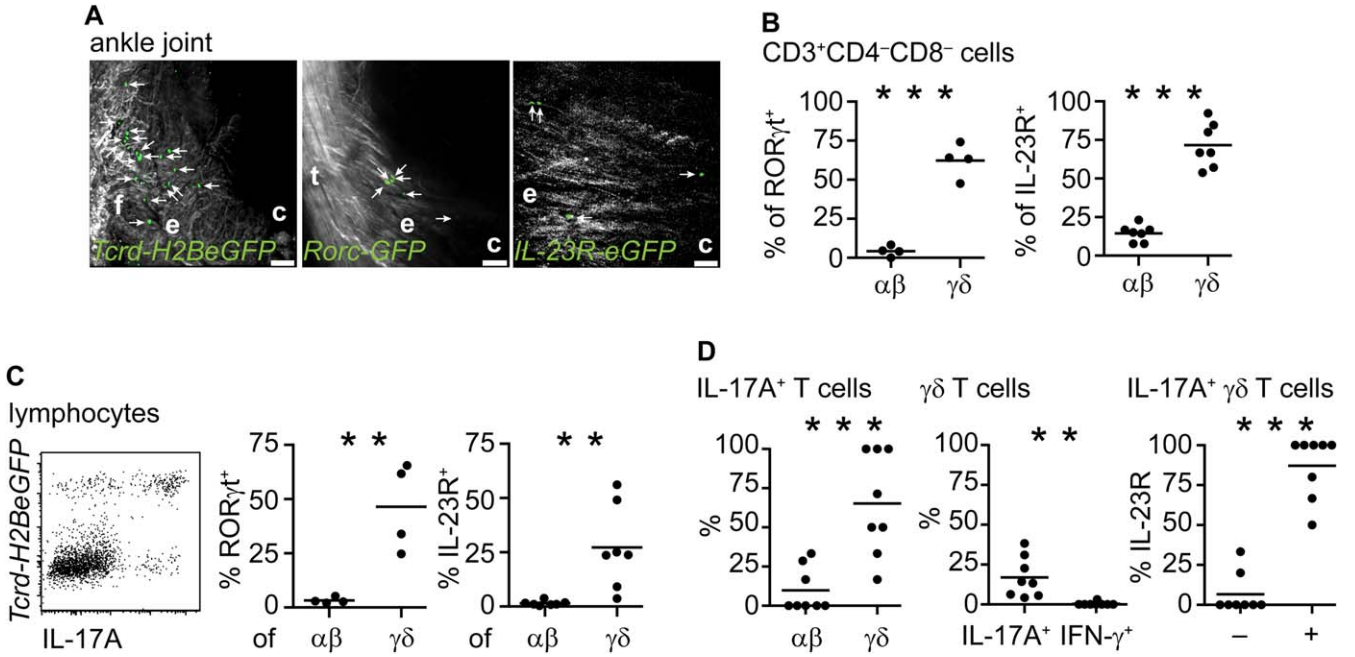

Figure 3. Enthesis-resident γ/δ T cells produce interleukin-17 (IL-17) and constitute the pool of retinoic acid receptor–related orphan nuclear receptor γt (RORγt)−positive and IL-23 receptor (IL-23R)−positive lymphocytes. **A**, Lateral views of *Tcrd-H2BeGFP, Rorc-GFP*, and *IL-23R-eGFP* mouse ankle joints analyzed ex vivo, obtained by 2-photon microscopy. **Arrows** show γ/δ T cells in the left panel, RORγt+ cells in the middle panel, and IL-23R+ cells in the right panel. Green indicates *Tcrd-H2BeGFP* in the left panel, *Rorc-GFP* in the middle panel, and *IL-23R-eGFP* in the right panel. White indicates collagen (second harmonic signal). **f** = fibrocartilage; **e** = enthesis; **c** = calcaneus; **t** = tendon. Bars = 50 μm. Images are representative of at least 2 mice per genotype. **B**−**D**, Results of flow cytometric analysis of entheses from *Tcrd-H2BeGFP*, *Rorc-GFP*, and *IL-23R-eGFP* mice. Cells were left unstimulated (**B**), stimulated with phorbol myristate acetate/ionomycin (**C**), or stimulated with IL-23 (**D**). **B**, Frequencies of α/β and γ/δ T cells among entheseal RORγt+ (left) and IL-23R+ (right) CD3+CD4−CD8− cells. **C**, IL-17 production by entheseal lymphocytes (left) and frequencies of RORγt+ (middle) and IL-23R+ (right) cells among α/β and γ/δ T cells. For IL-17 production, pooled data from 4 mice are shown. **D**, Frequencies of α/β and γ/δ T cells among entheseal IL-17−producing CD3+ cells (left), IL-17 production by entheseal γ/δ T cells (middle), and IL-23R expression by entheseal IL-17−producing γ/δ T cells (right). Symbols represent individual mice; horizontal lines show the mean. Data on *Rorc-GFP* mice are from 2 independent experiments; data on *Tcrd-H2BeGFP* mice and *IL-23R-eGFP* mice are from 4 independent experiments. ** = $P < 0.01$; *** = $P < 0.001$, by unpaired *t*-test.

is thus a site of γ/δ T cell enrichment. In absolute numbers, up to 200 entheseal γ/δ T cells could be isolated from 2 ankle joints from a naive mouse, all showing a CD4−CD8− phenotype characteristic of γ/δ T cells (Figure 1C and Supplementary Figure 2C). Typically, γ/δ T cells are classified according to expression of the variable domain of the TCRγ (Vγ) chain (26). At the Achilles tendon enthesis, some γ/δ T cells displayed Vγ1 or Vγ4 chains. However, the majority were Vγ6+ (Figure 1D) (nomenclature according to ref. 27), representing an IL-17−producing subset that is frequently found in the reproductive tract, lung, and dermis (26). Taken together, these data show that a population of nonmotile, tissue-resident Vγ6+ γ/δ T cells locates within the entheseal organs of various mouse joints.

Enthesis-resident γ/δ T cells show a preactivated effector phenotype. Next, we characterized enthesis-resident γ/δ T cells in more detail using flow cytometry of entheseal cell suspensions from *Tcrd-H2BeGFP* mice. Activated and functionally differentiated effector γ/δ T cells were shown to express high levels of CD44 (28). In naive mice, ~80% of all isolated enthesis-resident γ/δ T cells were $CD44^{high}$ (Figure 2A) and displayed a $CD44^{high}$CD62L− effector phenotype (Figure 2B). Since CCR6 (29) and CD27 (30) are surface markers for functional discrimination between IL-17−producing and IFNγ-producing γ/δ T cells, respectively, expression of both molecules on entheseal γ/δ T cells was determined (Figure 2B). At the enthesis, 40−80% of γ/δ T cells were preactivated $CD44^{high}$CCR6+ or $CD44^{high}$CD27− cells, suggesting IL-17 production capacity. Recently, Lombes and colleagues reported that analysis of CD44 together with Ly6C also allowed CD27− (CD44+Ly6C−) γ/δ T cells to be distinguished from CD27+ (CD44−Ly6C+ or CD44−Ly6C−) γ/δ T cells (31). Consistent with their and our previous findings, enthesis-resident γ/δ T cells were mainly

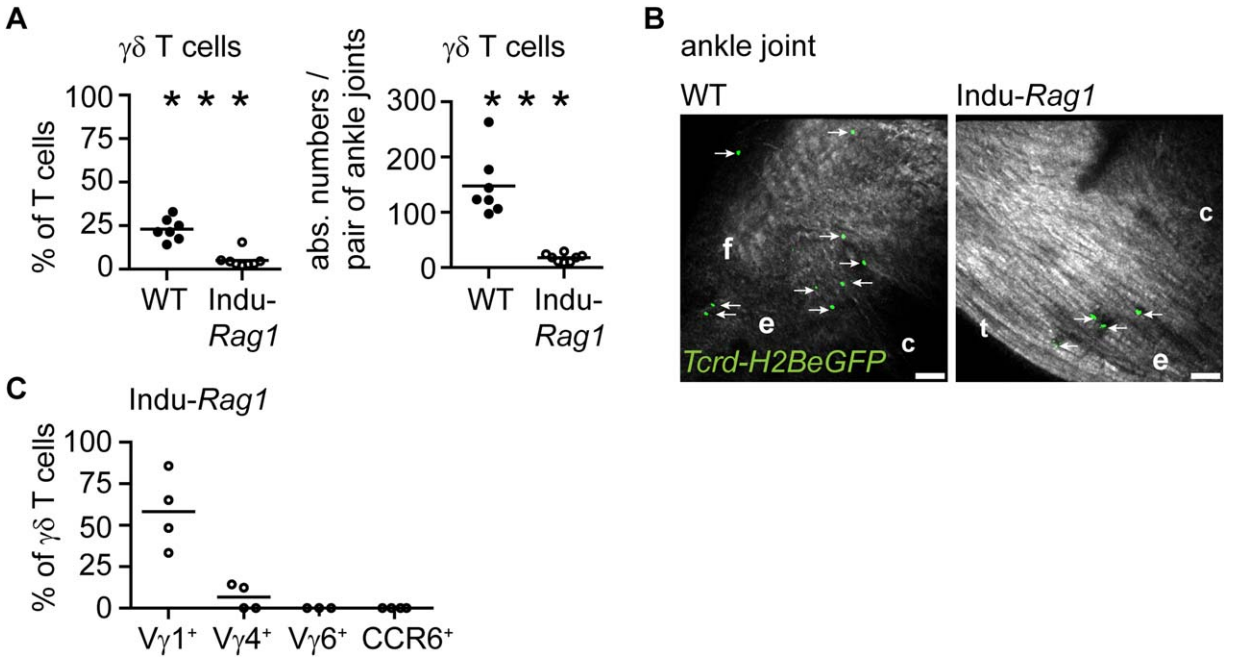

Figure 4. Dependence of entheseal γ/δ T cell development on an embryonic microenvironment. Enthesis-resident γ/δ T cells from age-matched wild-type (WT) *Tcrd-H2BeGFP* control mice and Indu-*Rag1* × *Tcrd-H2BeGFP* mice with lymphocyte development induced by tamoxifen were analyzed by flow cytometry and 2-photon microscopy 6−8 weeks after induction. **A**, Frequency of γ/δ T cells (left) and absolute (abs.) numbers of γ/δ T cells (right), as determined by flow cytometry. *** = $P < 0.001$ by unpaired *t*-test. **B**, Lateral views of the ankle joints of WT *Tcrd-H2BeGFP* mice (black) and Indu-*Rag1* mice (white) analyzed ex vivo, obtained by 2-photon microscopy. **Arrows** show γ/δ T cells, green indicates *Tcrd-H2BeGFP*, and white indicates collagen (second harmonic signal). **f** = fibrocartilage; **e** = enthesis; **c** = calcaneus; **t** = tendon. Bars = 50 μm. Images are representative of at least 4 mice per genotype. **C**, Results of flow cytometric analysis showing frequencies of γ/δ T cells expressing Vγ1, Vγ4, Vγ6, or CCR6 in tamoxifen-treated Indu-*Rag1* mice. In **A** and **C**, symbols represent individual mice; horizontal lines show the mean. Data are from 5 independent experiments in **A** and 4 independent experiments in **C**.

CD44+Ly6C− cells (Figure 2B). As expected, the large majority (>90%) of CD44^{high}CD62L− γ/δ T cells were Vγ6+CD27− cells (Figure 2B). In summary, the population of entheseal γ/δ T cells was dominated by Vγ6+CD44^{high}CD62L−Ly6C−CD27− activated effector memory cells.

Production of IL-17 at the enthesis by γ/δ T cells. Expression of retinoic acid receptor–related orphan nuclear receptor γt (RORγt) and IL-23R are hallmarks of IL-17−producing lymphocytes, including γ/δ T cells (32), Th17 cells (19,33), and group 3 innate lymphoid cells (34,35). To visualize the presence of RORγt+ and IL-23R+ cells within entheseal tissue, we next analyzed the Achilles tendon insertion into the posterior calcaneus of *Rorc-GFP* and *IL-23R-GFP* mice using 2-photon microscopy. In naive mice, we observed several RORγt+ enthesis-resident cells (Figure 3A), even though seemingly fewer than entheseal γ/δ T cells (Figure 3A). Consistent with the data published by Sherlock and colleagues (11), even fewer IL-23R+ cells were located at the enthesis (Figure 3A).

These findings prompted us to determine the abundance of IL-17A−producing RORγt+ and IL-23R+ cells among enthesis-resident lymphocytes by flow cytometry. The γ/δ T cells, but not α/β T cells, constituted the majority of all enthesis-resident RORγt+ and IL-23R+ T cells (Supplementary Figure 3A, available on the *Arthritis & Rheumatology* web site at http://onlinelibrary.wiley.com/doi/10.1002/art.39732/abstract) and more importantly, of the previously described CD3+CD4−CD8− cells (11) (Figure 3B). Our data also clearly show that H2BeGFP+ cells, thus γ/δ T cells, were the main IL-17A−producing RORγt+IL-23R+ entheseal cell type after in vitro stimulation with PMA/ionomycin (Figure 3C). Approximately 50% of enthesis-resident γ/δ T cells were RORγt+ (Figure 3C), and 25% were IL-23R+ (Figure 3C), with a majority of those cells being Vγ6+ (Supplementary Figure 3). As opposed to secondary lymphoid organs such as the spleen, where only 1.6% (32) of γ/δ T cells express IL-23R, but similar to the intestinal lamina propria, where 50−60% of γ/δ T cells were shown to be RORγt+ (19) or IL-23R+ (20), tissue-resident entheseal γ/δ T cells thus preferentially express RORγt and IL-23R.

Furthermore, γ/δ T cells significantly dominated the pool of IL-17−producing entheseal T cells after ex

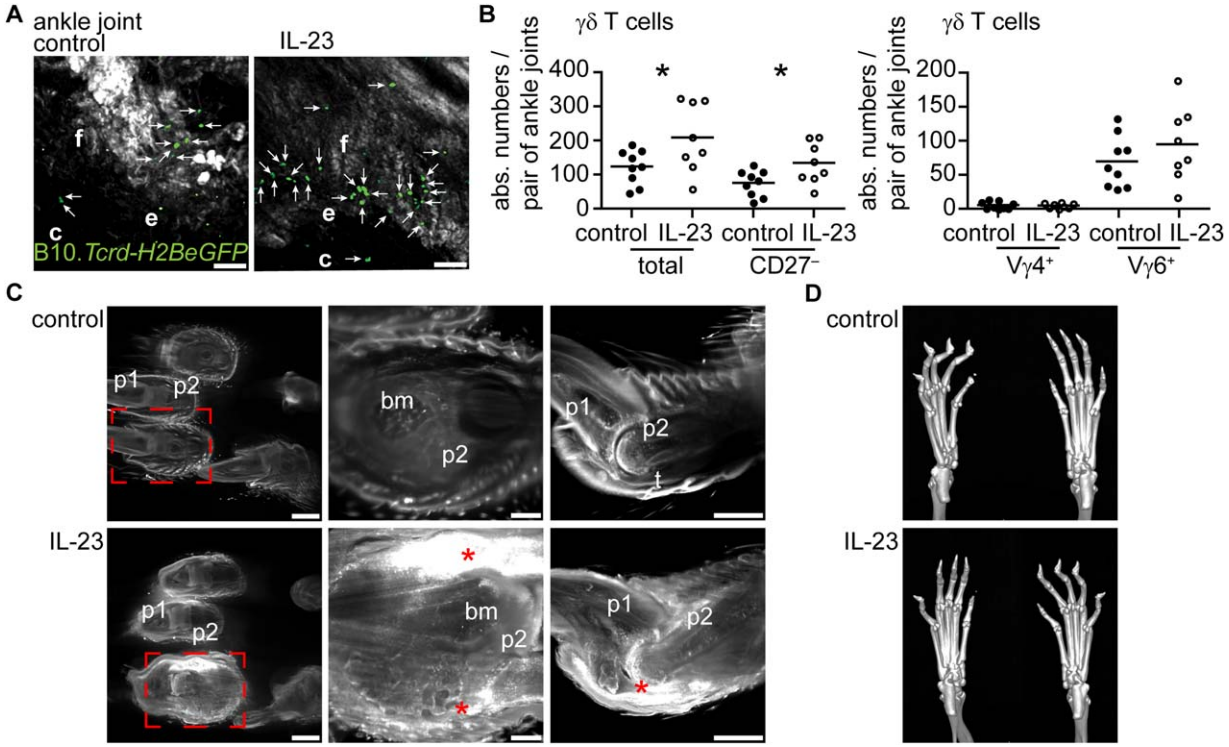

Figure 5. Accumulation of γ/δ T cells at the enthesis of ankle joints in mice overexpressing interleukin-23 (IL-23). B10.RIII *Tcrd-H2BeGFP* mice were hydrodynamically injected with control or IL-23 minicircle DNA. **A**, Posterior view of the mouse Achilles tendon enthesis obtained using 2-photon microscopy for ex vivo imaging. **Arrows** show γ/δ T cells, green indicates B10.*Tcrd-H2BeGFP*, and white indicates collagen (second harmonic signal). **c** = calcaneus; **e** = enthesis; **f** = fibrocartilage. Bars = 50 μm. Data are representative of 3 independent experiments with 3 control mice and 4 IL-23–overexpressing mice. **B**, Absolute (abs.) numbers of entheseal γ/δ T cells, as determined by flow cytometry. Symbols represent individual mice; horizontal lines show the mean. Data from 2 independent experiments are shown. * = $P < 0.05$ by unpaired *t*-test. **C**, Images of mouse paws obtained by light-sheet fluorescence microscopy. Plantar views (left) and lateral views (middle and right) are shown. Middle panels show a higher-magnification view of the boxed areas in the left panels. **Asterisks** indicate inflammation; white indicates autofluorescence. **bm** = bone marrow; **p1** = phalanx 1; **t** = tendon. Bars = 500 μm in the left panels, 200 μm in the middle panels, and 500 μm in the right panels. Images are representative of 5 independent experiments with 6 control mice and 10 IL-23–overexpressing mice. **D**, Micro–computed tomography images of mouse paws. Images are representative of 2 independent experiments with 4 control mice and 11 IL-23–overexpressing mice.

vivo stimulation with IL-23 only (Figure 3D). The majority of entheseal γ/δ T cells readily produced IL-17A after ex vivo stimulation, whereas only a minor population produced IFNγ (Figure 3D and Supplementary Figure 3). As expected, these enthesis-resident IL-17–producing γ/δ T cells were activated IL-23R+ cells (Figure 3D). Since enthesis-resident γ/δ T cells not only express key markers indicative of an IL-17–producing phenotype, but also possess the capacity to produce IL-17A ex vivo, they most likely represent the main IL-17–producing enthesis-resident lymphocyte population.

Enthesis-resident IL-17–producing γ/δ T cells are derived from fetal thymus. Functional development of mouse γ/δ T cells is believed to occur in distinct waves during fetal, neonatal, and adult thymopoiesis (28). Here, we investigated the ontogeny of enthesis-resident γ/δ T cells using inducible *Rag1*$^{-/-}$ (22) mice that were crossed to *Tcrd-H2BeGFP* mice (here termed Indu-*Rag1* mice). These mice lack lymphocyte development until induction with tamoxifen at a defined time point (21). Importantly, immunologic side effects are not expected after nonrecurring low-dose administration of tamoxifen. As determined by flow cytometry up to 8 weeks after induction, the proportion of γ/δ T cells was significantly decreased in tamoxifen-treated Indu-*Rag1* mice compared to 8-week-old wild-type *Tcrd-H2BeGFP* mice (Figure 4A). Also, absolute numbers were strongly reduced in tamoxifen-treated Indu-*Rag1* mice (Figure 4A). A severe reduction in entheseal γ/δ T cells in tamoxifen-treated Indu-*Rag1* mice was also observed by two-photon microscopy (Figure 4B).

Using the Indu-*Rag1* mouse model, Haas and colleagues previously showed that IL-17–producing γ/δ T cells developed exclusively before birth (21). Consistent

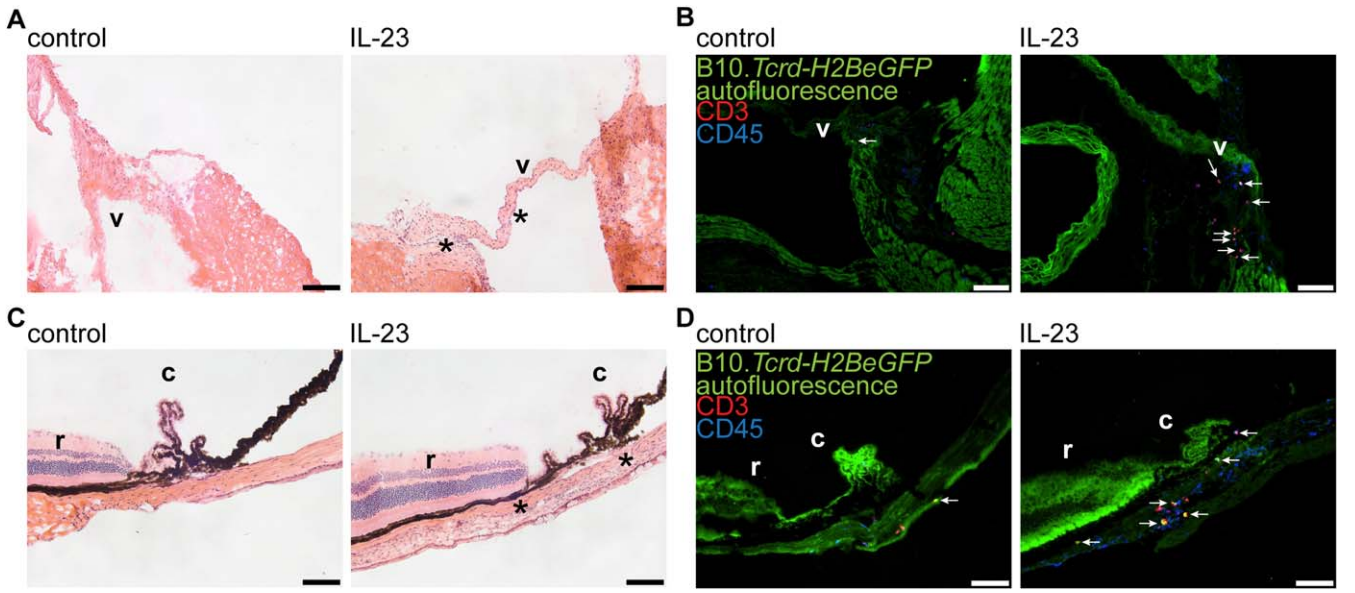

Figure 6. Accumulation of γ/δ T cells at the aortic root and within the eye in mice overexpressing interleukin-23 (IL-23). B10.RIII *Tcrd-H2BeGFP* mice were hydrodynamically injected with control or IL-23 minicircle DNA. **A** and **B**, Hematoxylin and eosin (H&E) (**A**) and immunofluorescence (**B**) staining of a mouse heart. **C** and **D**, H&E (**C**) and immunofluorescence (**D**) staining of a mouse eye. **Arrows** show γ/δ T cells, **asterisks** indicate inflammation, green indicates autofluorescence (B10.*Tcrd-H2BeGFP*), red indicates T cells (CD3), and blue indicates lymphocytes (CD45). **v** = valve; **c** = ciliary body; **r** = retina. Bars = 100 μm. Images in **A** and **B** are representative of 6 independent experiments; images in **C** and **D** are representative of 5 independent experiments, with 6–7 control mice and 10–11 IL-23–overexpressing mice.

with the findings of that study, enthesis-resident Vγ6+ or CCR6+ γ/δ T cells, which are known to be IL-17 producers, were completely absent in tamoxifen-treated Indu-*Rag1* mice (Figure 4C). As expected, few Vγ1+ or Vγ4+ entheseal γ/δ T cells developed in an adult microenvironment (Figure 4C). Taken together, our data indicate that the development of enthesis-resident IL-17–producing γ/δ T cells depends on an embryonic microenvironment and that these cells are later maintained as self-renewing tissue-resident cells.

Accumulation of entheseal γ/δ T cells at the Achilles tendon enthesis in mice overexpressing IL-23. To study entheseal γ/δ T cells in IL-23 minicircle–induced inflammation, we first backcrossed C57BL/6 *Tcrd-H2BeGFP* mice to the susceptible B10.RIII background. Using hydrodynamic injection, we introduced an IL-23–encoding minicircle DNA construct into B10.RIII mice. Overexpression of IL-23 in these mice leads to increased serum levels of IL-23, specifically inducing joint-destructive arthritis and severe bone loss (36) as well as typical features of SpA, including enthesitis and new bone formation (11). A control group was injected with an empty control minicircle DNA construct.

Importantly, in vivo, increased serum levels of IL-23 protein, accompanied by entheseal inflammation, were detected in IL-23 minicircle–injected B10.RIII *Tcrd-H2BeGFP* mice (see Supplementary Figure 4, available on the *Arthritis & Rheumatology* web site at http://onlinelibrary.wiley.com/doi/10.1002/art.39732/abstract), affirming the specific functional role of IL-23 in enthesitis. Using 2-photon microscopy, we observed an accumulation of enthesis-resident γ/δ T cells in mice overexpressing IL-23 (Figure 5A). Also, significantly higher numbers of γ/δ T cells, specifically CD27− γ/δ T cells, were isolated from the entheseal tissue of IL-23 minicircle–injected mice (Figure 5B). The increased presence of entheseal γ/δ T cells was most likely due to expansion of IL-17–producing Vγ6+, but not Vγ4+, γ/δ T cells (Figure 5B).

Next, we used light-sheet fluorescence microscopy of optically cleared paws as a novel read-out that allowed us to precisely visualize enthesitis with inflammatory infiltrates adjacent to interphalangeal joints (Figure 5C and Supplementary Video 2, available on the *Arthritis & Rheumatology* web site at http://onlinelibrary.wiley.com/doi/10.1002/art.39732/abstract). As monitored by micro-CT, the alterations observed by light-sheet fluorescence microscopy preceded obvious bone remodeling (Figures 5C and D), a hallmark of SpA (37). Taken together, these data suggest a contribution of preactivated IL-17–producing CD27−IL-23R+ entheseal γ/δ T cells to inflammatory processes involved in enthesitis.

Accumulation of γ/δ T cells in the eye and the aortic valve in mice overexpressing IL-23. Mice with arthritic paw inflammation further developed mild psoriatic skin lesions with epidermal thickening (Supplementary Figure 4B) and aortic valve inflammation (Figure 6A), which is consistent with previous findings in mice (11) and humans (1,2). Notably, we observed that γ/δ T cells accumulated not only within the entheseal tissue in joints (Figures 5A and B), but also at the aortic valve and root (Figure 6B), further extending their enthesitis-promoting potential. In addition, SpA patients are at risk of developing uveitis (1). In this study, mice overexpressing IL-23 displayed lymphocyte infiltrations within the uvea, with γ/δ T cell accumulations adjacent to the ciliary body (Figures 6C and D). In summary, we demonstrated that entheseal γ/δ T cells are not confined to joints, but they also reside in distinct anatomic niches at the aortic valve and the uvea, where they accumulate in an IL-23–dependent manner.

DISCUSSION

To date, drug treatment of SpA has been based on blockade of tumor necrosis factor (TNF) or the use of nonsteroidal antiinflammatory drugs (NSAIDs), leading to effective reduction in chronic inflammation and pain. For a long time, it was thought that these therapies were not capable of reducing and inhibiting radiographic progression, leading to entheseal new bone formation and impaired mobility (37). Data acquired in a large longitudinal study, however, demonstrated reduced axial progression in AS patients treated with TNF inhibitors (38). Since some patients do not respond to either TNF blockers or NSAIDs, there is still a need for alternative therapies. In recent years, several studies have identified involvement of the IL-23/IL-17 cytokine axis in the pathology of SpA (6). The first clinical trials using anti–IL-17A antibodies for the treatment of AS, rheumatoid arthritis (RA), psoriasis, or uveitis, anti–IL-17R for the treatment of psoriatic arthritis, anti–IL-23/IL-12p40 antibodies for the treatment of AS or psoriatic arthritis, and anti–IL-23p19 antibodies for the treatment of AS (ongoing trial) have been performed, mainly yielding promising results (39). Notably, the cellular sources of these proinflammatory cytokines remain unclear and are a subject of controversy (6). Since data regarding human entheseal cell infiltrates are limited, the use of animal models with features of human SpA is very important to reveal pathways and cell types that might be involved in the inflammatory pathogenesis of enthesitis and ossification of entheseal tissues.

In the inflamed joints of mice with collagen-induced arthritis, a mouse model resembling human RA, γ/δ T cells were identified as important (40) or main (41) producers of IL-17. Vγ4+ IL-17–producing γ/δ T cells were believed to exacerbate collagen-induced arthritis (40). Recently, in an experimental mouse model of autoimmune arthritis, a population of pathogenic Vγ6+CCR2+ IL-17–producing γ/δ T cells was described within the joints (42). An IL-17–producing γ/δ T cell population was also observed in mannan-induced psoriatic arthritis–like disease, causing arthritis joint inflammation as well as psoriatic lesions of the skin (43). In contrast to our findings, both of these recently described IL-17–producing γ/δ T cell populations were not tissue resident but immigrated from draining lymph nodes upon inflammatory stimulation. This further highlights an exceptional tissue-specific role of enthesis-resident γ/δ T cells. In particular, the physiologic role of Vγ6+ IL-17–producing γ/δ T cells in healthy animals still requires further investigation. This might include bone remodeling, adaptation, and regeneration in response to mechanical stress.

So far, only a few studies have analyzed γ/δ T cells in SpA patients. Two recent studies showed an enrichment of IL-17–producing or even IL-23R+ IL-17–producing γ/δ T cells within the peripheral blood of patients with enthesitis-related arthritis (13) or AS (17), respectively. The presence of γ/δ T cells within the inflamed synovia of patients with RA or juvenile idiopathic arthritis has also been observed, although data about their pathogenic potential were a subject of controversy (44,45).

Entheseal organs are permanently exposed to mechanical forces and microdamage and are hence constantly switching between anabolic and catabolic processes. Thus, it is conceivable that enthesis-resident γ/δ T cells interfere with bone metabolism to control tissue homeostasis in rodents and humans. Jacques and colleagues identified the importance of biomechanical stress in the induction of enthesitis in mice, as hind limb unloading prevented enthesitis in generally highly susceptible TNF-transgenic mice (46). Since tissue-resident γ/δ T cells within the skin or intestines are known to rapidly respond to either cytokine stimulation or stromal and epithelial cell stress-induced molecules, one could speculate that entheseal microdamage could activate enthesis-resident γ/δ T cells and trigger production of proinflammatory cytokines such as IL-17A. Whether genetic factors including HLA–B27 or polymorphisms in the IL-23R decrease the threshold for microdamage-induced γ/δ T cell activation or just alter activated γ/δ T cell responses remains an important open question (47).

Given the fact that our data reveal an accumulation of γ/δ T cells not just in joint entheseal regions, but adjacent to the ciliary body in the eye as well as along the

aortic valve and root, it appears likely that accumulation of γ/δ T cells in different enthesis-related tissues reveals a common IL-23–driven mechanism. In humans, SpA pathologies include inflammation of gut or skin, sites which were shown in mice to contain high numbers of IL-23R+ γ/δ T cells (20,48). Using systemic administration of β-glucan to SKG mice as a suitable SpA model, the gut was demonstrated to be the main site of IL-23 production in experimental SpA (49). Also, a relationship between host microbiota and arthritis onset and severity was reported in mice (49). In fact, elevated IL-23 levels were found in ileal biopsy specimens from SpA patients (10), thus proposing the gut as a key producer of excessive IL-23 in human SpA. Further, it is conceivable that the microbiome is crucially involved in the IL-23–dependent pathogenesis of human SpA (50).

In conclusion, we propose that entheseal γ/δ T cells are key players controlling tissue homeostasis at tendon-to-bone attachment sites. The γ/δ T cells are the main IL-17–producing cell type within the enthesis-resident lymphocyte population and within the pool of RORγt+IL-23R+CD3+CD4−CD8− lymphocytes. We demonstrate that entheseal γ/δ T cells accumulate at anatomic sites that are affected during SpA, such as the Achilles tendon insertion, the aortic root, and the ciliary body.

ACKNOWLEDGMENTS

We thank Matthias Lochner and Gérard Eberl for providing *Rorc-GFP* mice. We thank all members of the DFG priority program SPP1468 ImmunoBone for support and fruitful discussions.

AUTHOR CONTRIBUTIONS

All authors were involved in drafting the article or revising it critically for important intellectual content, and all authors approved the final version to be published. Dr. Prinz had full access to all of the data in the study and takes responsibility for the integrity of the data and the accuracy of the data analysis.

Study conception and design. Reinhardt, Korn, Weiss, Förster, Prinz.

Acquisition of data. Reinhardt, Yevsa, Worbs, Lienenklaus, Sandrock, Oberdörfer, Prinz.

Analysis and interpretation of data. Reinhardt, Worbs, Lienenklaus, Sandrock, Prinz.

REFERENCES

1. Stolwijk C, van Tubergen A, Castillo-Ortiz JD, Boonen A. Prevalence of extra-articular manifestations in patients with ankylosing spondylitis: a systematic review and meta-analysis. Ann Rheum Dis 2015;74:65–73.
2. Roldan CA, Chavez J, Wiest PW, Qualls CR, Crawford MH. Aortic root disease and valve disease associated with ankylosing spondylitis. J Am Coll Cardiol 1998;32:1397–404.
3. Cortes A, Hadler J, Pointon JP, Robinson PC, Karaderi T, Leo P, et al. Identification of multiple risk variants for ankylosing spondylitis through high-density genotyping of immune-related loci. Nat Genet 2013;45:730–8.
4. Cargill M, Schrodi SJ, Chang M, Garcia VE, Brandon R, Callis KP, et al. A large-scale genetic association study confirms IL12B and leads to the identification of IL23R as psoriasis-risk genes. Am J Hum Genet 2007;80:273–90.
5. Duerr RH, Taylor KD, Brant SR, Rioux JD, Silverberg MS, Daly MJ, et al. A genome-wide association study identifies IL23R as an inflammatory bowel disease gene. Science 2006;314:1461–3.
6. Lubberts E. The IL-23-IL-17 axis in inflammatory arthritis. Nat Rev Rheumatol 2015;11:415–29.
7. DeLay ML, Turner MJ, Klenk EI, Smith JA, Sowders DP, Colbert RA. HLA–B27 misfolding and the unfolded protein response augment interleukin-23 production and are associated with Th17 activation in transgenic rats. Arthritis Rheum 2009;60:2633–43.
8. Ciccia F, Accardo-Palumbo A, Rizzo A, Guggino G, Raimondo S, Giardina A, et al. Evidence that autophagy, but not the unfolded protein response, regulates the expression of IL-23 in the gut of patients with ankylosing spondylitis and subclinical gut inflammation. Ann Rheum Dis 2014;73:1566–74.
9. Mei Y, Pan F, Gao J, Ge R, Duan Z, Zeng Z, et al. Increased serum IL-17 and IL-23 in the patient with ankylosing spondylitis. Clin Rheumatol 2011;30:269–73.
10. Ciccia F, Bombardieri M, Principato A, Giardina A, Tripodo C, Porcasi R, et al. Overexpression of interleukin-23, but not interleukin-17, as an immunologic signature of subclinical intestinal inflammation in ankylosing spondylitis. Arthritis Rheum 2009;60:955–65.
11. Sherlock JP, Joyce-Shaikh B, Turner SP, Chao CC, Sathe M, Grein J, et al. IL-23 induces spondyloarthropathy by acting on ROR-γt+ CD3+CD4−CD8− entheseal resident T cells. Nat Med 2012;18:1069–76.
12. Shen H, Goodall JC, Hill Gaston JS. Frequency and phenotype of peripheral blood Th17 cells in ankylosing spondylitis and rheumatoid arthritis. Arthritis Rheum 2009;60:1647–56.
13. Gaur P, Misra R, Aggarwal A. Natural killer cells and γ-δ T cell alterations in enthesitis related arthritis category of juvenile idiopathic arthritis. Clin Immunol 2015;161:163–9.
14. Laloux L, Voisin MC, Allain J, Martin N, Kerboull L, Chevalier X, et al. Immunohistological study of entheses in spondyloarthropathies: comparison in rheumatoid arthritis and osteoarthritis. Ann Rheum Dis 2001;60:316–21.
15. McGonagle D, Marzo-Ortega H, O'Connor P, Gibbon W, Hawkey P, Henshaw K, et al. Histological assessment of the early enthesitis lesion in spondyloarthropathy. Ann Rheum Dis 2002;61:534–7.
16. Noordenbos T, Yeremenko N, Gofita I, van de Sande M, Tak PP, Canete JD, et al. Interleukin-17–positive mast cells contribute to synovial inflammation in spondylarthritis. Arthritis Rheum 2012;64:99–109.
17. Kenna TJ, Davidson SI, Duan R, Bradbury LA, McFarlane J, Smith M, et al. Enrichment of circulating interleukin-17–secreting interleukin-23 receptor–positive γ/δ T cells in patients with active ankylosing spondylitis. Arthritis Rheum 2012;64:1420–9.
18. Prinz I, Sansoni A, Kissenpfennig A, Ardouin L, Malissen M, Malissen B. Visualization of the earliest steps of γδ T cell development in the adult thymus. Nat Immunol 2006;7:995–1003.
19. Lochner M, Peduto L, Cherrier M, Sawa S, Langa F, Varona R, et al. In vivo equilibrium of proinflammatory IL-17+ and regulatory IL-10+ Foxp3+ RORγt+ T cells. J Exp Med 2008;205:1381–93.
20. Awasthi A, Riol-Blanco L, Jager A, Korn T, Pot C, Galileos G, et al. Cutting edge: IL-23 receptor gfp reporter mice reveal distinct populations of IL-17–producing cells. J Immunol 2009;182:5904–8.
21. Haas JD, Ravens S, Duber S, Sandrock I, Oberdorfer L, Kashani E, et al. Development of interleukin-17-producing γδ T cells is restricted to a functional embryonic wave. Immunity 2012;37:48–59.

22. Duber S, Hafner M, Krey M, Lienenklaus S, Roy B, Hobeika E, et al. Induction of B-cell development in adult mice reveals the ability of bone marrow to produce B-1a cells. Blood 2009;114:4960–7.
23. Roark CL, Aydintug MK, Lewis J, Yin X, Lahn M, Hahn YS, et al. Subset-specific, uniform activation among Vγ6/Vδ1+γδ T cells elicited by inflammation. J Leukoc Biol 2004;75:68–75.
24. Ertürk A, Becker K, Jahrling N, Mauch CP, Hojer CD, Egen JG, et al. Three-dimensional imaging of solvent-cleared organs using 3DISCO. Nat Protoc 2012;7:1983–95.
25. Reinhardt A, Ravens S, Fleige H, Haas JD, Oberdorfer L, Lyszkiewicz M, et al. CCR7-mediated migration in the thymus controls γδ T-cell development. Eur J Immunol 2014;44:1320–9.
26. Carding SR, Egan PJ. Gammadelta T cells: functional plasticity and heterogeneity. Nat Rev Immunol 2002;2:336–45.
27. Heilig JS, Tonegawa S. Diversity of murine γ genes and expression in fetal and adult T lymphocytes. Nature 1986;322:836–40.
28. Prinz I, Silva-Santos B, Pennington DJ. Functional development of γδ T cells. Eur J Immunol 2013;43:1988–94.
29. Haas JD, Gonzalez FH, Schmitz S, Chennupati V, Fohse L, Kremmer E, et al. CCR6 and NK1.1 distinguish between IL-17A and IFN-γ-producing γδ effector T cells. Eur J Immunol 2009; 39:3488–97.
30. Ribot JC, deBarros A, Pang DJ, Neves JF, Peperzak V, Roberts SJ, et al. CD27 is a thymic determinant of the balance between interferon-γ- and interleukin 17-producing γδ T cell subsets. Nat Immunol 2009;10:427–36.
31. Lombes A, Durand A, Charvet C, Riviere M, Bonilla N, Auffray C, et al. Adaptive immune-like γ/δ T lymphocytes share many common features with their α/β T cell counterparts. J Immunol 2015;195:1449–58.
32. Sutton CE, Lalor SJ, Sweeney CM, Brereton CF, Lavelle EC, Mills KH. Interleukin-1 and IL-23 induce innate IL-17 production from γδ T cells, amplifying Th17 responses and autoimmunity. Immunity 2009;31:331–41.
33. Zhou L, Ivanov, II, Spolski R, Min R, Shenderov K, Egawa T, et al. IL-6 programs T(H)−17 cell differentiation by promoting sequential engagement of the IL-21 and IL-23 pathways. Nat Immunol 2007;8:967–74.
34. Sawa S, Cherrier M, Lochner M, Satoh-Takayama N, Fehling HJ, Langa F, et al. Lineage relationship analysis of RORγt+ innate lymphoid cells. Science 2010;330:665–9.
35. Takatori H, Kanno Y, Watford WT, Tato CM, Weiss G, Ivanov II, et al. Lymphoid tissue inducer-like cells are an innate source of IL-17 and IL-22. J Exp Med 2009;206:35–41.
36. Adamopoulos IE, Tessmer M, Chao CC, Adda S, Gorman D, Petro M, et al. IL-23 is critical for induction of arthritis, osteoclast formation, and maintenance of bone mass. J Immunol 2011;187:951–9.
37. Lories RJ, Haroon N. Bone formation in axial spondyloarthritis. Best Pract Res Clin Rheumatol 2014;28:765–77.
38. Haroon N, Inman RD, Learch TJ, Weisman MH, Lee M, Rahbar MH, et al. The impact of tumor necrosis factor α inhibitors on radiographic progression in ankylosing spondylitis. Arthritis Rheum 2013;65:2645–54.
39. Gaffen SL, Jain R, Garg AV, Cua DJ. The IL-23-IL-17 immune axis: from mechanisms to therapeutic testing. Nat Rev Immunol 2014;14:585–600.
40. Roark CL, French JD, Taylor MA, Bendele AM, Born WK, O'Brien RL. Exacerbation of collagen-induced arthritis by oligoclonal, IL-17-producing γδ T cells. J Immunol 2007;179:5576–83.
41. Ito Y, Usui T, Kobayashi S, Iguchi-Hashimoto M, Ito H, Yoshitomi H, et al. Gamma/delta T cells are the predominant source of interleukin-17 in affected joints in collagen-induced arthritis, but not in rheumatoid arthritis. Arthritis Rheum 2009; 60:2294–303.
42. Akitsu A, Ishigame H, Kakuta S, Chung SH, Ikeda S, Shimizu K, et al. IL-1 receptor antagonist-deficient mice develop autoimmune arthritis due to intrinsic activation of IL-17-producing CCR2(+)Vγ6(+)γδ T cells. Nat Commun 2015;6:7464.
43. Khmaladze I, Kelkka T, Guerard S, Wing K, Pizzolla A, Saxena A, et al. Mannan induces ROS-regulated, IL-17A-dependent psoriasis arthritis-like disease in mice. Proc Natl Acad Sci U S A 2014;111:E3669–78.
44. Shen Y, Li S, Quayle AJ, Mellbye OJ, Natvig JB, Forre O. TCR γ/δ+ cell subsets in the synovial membranes of patients with rheumatoid arthritis and juvenile rheumatoid arthritis. Scand J Immunol 1992;36:533–40.
45. Berkun Y, Bendersky A, Gerstein M, Goldstein I, Padeh S, Bank I. Gammadelta T cells in juvenile idiopathic arthritis: higher percentages of synovial Vδ1+ and Vγ9+ T cell subsets are associated with milder disease. J Rheumatol 2011;38:1123–9.
46. Jacques P, Lambrecht S, Verheugen E, Pauwels E, Kollias G, Armaka M, et al. Proof of concept: enthesitis and new bone formation in spondyloarthritis are driven by mechanical strain and stromal cells. Ann Rheum Dis 2014;73:437–45.
47. McGonagle D, Thomas RC, Schett G. Spondyloarthritis: may the force be with you? Ann Rheum Dis 2014;73:321–3.
48. Cai Y, Shen X, Ding C, Qi C, Li K, Li X, et al. Pivotal role of dermal IL-17-producing γδ T cells in skin inflammation. Immunity 2011;35:596–610.
49. Rehaume LM, Mondot S, Aguirre de Carcer D, Velasco J, Benham H, Hasnain SZ, et al. ZAP-70 genotype disrupts the relationship between microbiota and host, leading to spondyloarthritis and ileitis in SKG mice. Arthritis Rheumatol 2014;66:2780–92.
50. Costello ME, Ciccia F, Willner D, Warrington N, Robinson PC, Gardiner B, et al. Intestinal dysbiosis in ankylosing spondylitis. Arthritis Rheumatol 2015;67:686–91.